# 44

# ON SOME POSSIBILITIES OF CREATION OF HYPERSONIC FLOWS IN WIND TUNNELS

A. A. Nikolsky

Academy of Sciences, U.S.S.R.

## PART I

### HYPERSONIC NOZZLES WITH NONUNIFORM POTENTIAL FLOW IN TEST SECTION

Analogy between hypersonic steady gas motions and unsteady gas motions in a space of small dimensions is established in various papers.[1-4] All conclusions are directed to the investigation of a case of the hypersonic flow about slender bodies; the transformation of motion equations and boundary conditions are carried out together. The analysis includes typical, specific flow values, and a Mach number of the undisturbed flow and thickness ratio of a body. It is not clearly formulated in these considerations that not only in the hypersonic flow about bodies but generally in any steady hypersonic flows—particularly in hypersonic flows in ducts—there is an approximate analogy with unsteady flows of smaller dimensions where everywhere in the flow region the direction of the velocity vector differs but slightly from some fixed direction.

In the present paper a demonstration of the above-mentioned analogy is given which indicates that this analogy is rather accurate even in flows with local Mach number $= 3$.

The application of this analogy permits the use of some unsteady motions for the approximate creation of original hypersonic flows in nozzles. In case of two-dimensional irrotational hypersonic flows, the given analogy with unsteady motions exists in the general case even if the velocity vector inclination angle varies greatly in the flow region. The conclusion of this analogy is given herein.

The equation system of the steady adiabatic gas motion has the form

$$u \frac{\partial u}{\partial x} + v \frac{\partial u}{\partial y} + w \frac{\partial u}{\partial z} = - \frac{1}{\rho} \frac{\partial p}{\partial x} \tag{1}$$

$$u \frac{\partial v}{\partial x} + v \frac{\partial v}{\partial y} + w \frac{\partial v}{\partial z} = -\frac{1}{\rho} \frac{\partial p}{\partial y} \tag{2}$$

$$u \frac{\partial w}{\partial x} + v \frac{\partial w}{\partial y} + w \frac{\partial w}{\partial z} = -\frac{1}{\rho} \frac{\partial p}{\partial z} \tag{3}$$

$$u \frac{\partial}{\partial x} \left( \frac{p}{\rho^{\varkappa}} \right) + v \frac{\partial}{\partial y} \left( \frac{p}{\rho^{\varkappa}} \right) + w \frac{\partial}{\partial z} \left( \frac{p}{\rho^{\varkappa}} \right) = 0 \tag{4}$$

$$\frac{\partial(\rho u)}{\partial x} + \frac{\partial(\rho v)}{\partial y} + \frac{\partial(\rho w)}{\partial z} = 0 \tag{5}$$

where $u$, $v$, $w$ are components of the velocity vector along axes $x$, $y$, $z$, $p$ = pressure, $\rho$ = density, $\varkappa$ = specific heat ratio of gas. Equations (1)–(4) show that the enthalpy $i_0$ is constant along with stream lines.

$$i_0 = \frac{u^2 + v^2 + w^2}{2} + \frac{\varkappa}{\varkappa - 1} \frac{p}{\rho} = \text{Const.} \tag{6}$$

Consider the motions when $i_0$ is constant in the whole flow region. Then if the motion is hypersonic, the value $V = \sqrt{u^2 + v^2 + w^2}$ of the velocity vector modulus in the whole flow region nears its maximum value, then maximum velocity $V_{\max} = \sqrt{2i_0}$. Transform Eq. (5) to the form

$$\frac{\partial \ln (\rho V)}{\partial \varsigma} + \frac{\partial \cos \alpha}{\partial x} + \frac{\partial \cos \beta}{\partial y} + \frac{\partial \cos \gamma}{\partial z} = 0 \tag{7}$$

where $\alpha$, $\rho$, $\gamma$ are angles between the velocity vector and $x$, $y$, $z$ axes, and $\partial/\partial\varsigma = \cos \alpha(\partial/\partial x) + \cos \beta(\partial/\partial y) + \cos \gamma(\partial/\partial z)$ is the derivative along the stream line. As it is seen from Eq. (4) $\theta = p/\rho(1/\varkappa)$ is constant value along the streamlines. Using this fact and Eq. (6) we shall have that along the streamlines the differential equality

$$\frac{d \ln V}{d \ln \rho} = -\frac{\varkappa \frac{p}{\varsigma}}{V^2} = -\frac{1}{M^2} \tag{8}$$

is valid where $M$ is local Mach number. Using this relation, represent the first term of the left-hand side of Eq. (7) in the form

$$\frac{\partial}{\partial \varsigma} \ln (\rho V) = \left( 1 - \frac{1}{M^2} \right) \frac{\partial}{\partial \varsigma} \ln \rho \tag{9}$$

At high $M$ numbers the value $M^{-2}$ is small in comparison with a unit. Even at not very high $M = 3$ it is 9 times less than a unit, i.e., by the order is less than a unit.

Omitting the value as compared to a unit, write Eq. (7) in the form, typical for arbitrary hypersonic motions:

$$\frac{\partial \ln \rho}{\partial \zeta} + \frac{\partial \cos \alpha}{\partial x} + \frac{\partial \cos \beta}{\partial y} + \frac{\partial \cos \gamma}{\partial z} = 0 \tag{10}$$

Equations (1)–(3) may be presented in the form

$$\cos \alpha \frac{\partial \ln V}{\partial \zeta} + \frac{\partial \cos \alpha}{\partial \zeta} = - \frac{1}{\rho V^2} \frac{\partial p}{\partial x} \tag{11}$$

$$\cos \beta \frac{\partial \ln V}{\partial \zeta} + \frac{\partial \cos \beta}{\partial \zeta} = - \frac{1}{\rho V^2} \frac{\partial p}{\partial y} \tag{12}$$

$$\cos \gamma \frac{\partial \ln V}{\partial \zeta} + \frac{\partial \cos \gamma}{\partial \zeta} = - \frac{1}{\rho V^2} \frac{\partial p}{\partial z} \tag{13}$$

Using the relation [Eq. (8)] write the equations in the form

$$- \frac{1}{M^2} \cos \alpha \frac{\partial \ln \rho}{\partial \zeta} + \frac{\partial \cos \alpha}{\partial \zeta} = - \frac{1}{\rho V^2} \frac{\partial p}{\partial x}$$

$$- \frac{1}{M^2} \cos \beta \frac{\partial \ln \rho}{\partial \zeta} + \frac{\partial \cos \beta}{\partial \zeta} = - \frac{1}{\rho V^2} \frac{\partial p}{\partial y}$$

$$- \frac{1}{M^2} \cos \gamma \frac{\partial \ln \rho}{\partial \zeta} + \frac{\partial \cos \gamma}{\partial \zeta} = - \frac{1}{\rho V^2} \frac{\partial p}{\partial z}$$

Changing the derivative of the density from Eq. (10) we have

$$\frac{1}{M^2} \cos \alpha \left( \frac{\partial \cos \alpha}{\partial x} + \frac{\partial \cos \beta}{\partial y} + \frac{\partial \cos \gamma}{\partial z} \right) + \cos \alpha \frac{\partial \cos \alpha}{\partial x}$$
$$+ \cos \beta \frac{\partial \cos \alpha}{\partial y} + \cos \gamma \frac{\partial \cos \alpha}{\partial z} = - \frac{1}{\rho V^2} \frac{\partial p}{\partial x} \tag{14}$$

$$\frac{1}{M^2} \cos \beta \left( \frac{\partial \cos \alpha}{\partial x} + \frac{\partial \cos \beta}{\partial y} + \frac{\partial \cos \gamma}{\partial z} \right) + \cos \alpha \frac{\partial \cos \beta}{\partial x}$$
$$+ \cos \beta \frac{\partial \cos \beta}{\partial y} + \cos \gamma \frac{\partial \cos \beta}{\partial z} = - \frac{1}{\rho V^2} \frac{\partial p}{\partial y} \tag{15}$$

$$\frac{1}{M^2} \cos \gamma \left( \frac{\partial \cos \alpha}{\partial x} + \frac{\partial \cos \beta}{\partial y} + \frac{\partial \cos \gamma}{\partial z} \right) + \cos \alpha \frac{\partial \cos \gamma}{\partial x}$$
$$+ \cos \beta \frac{\partial \cos \gamma}{\partial y} + \cos \gamma \frac{\partial \cos \gamma}{\partial z} = - \frac{1}{\rho V^2} \frac{\partial p}{\partial z} \tag{16}$$

At high $M$ numbers the first terms of the left-hand side of these equations disappear and the equations are presented in the form

$$\cos \alpha \, \frac{\partial \cos \alpha}{\partial x} + \cos \beta \, \frac{\partial \cos \alpha}{\partial y} + \cos \gamma \, \frac{\partial \cos \alpha}{\partial z} = -\frac{1}{\rho V^2} \frac{\partial p}{\partial x} \tag{17}$$

$$\cos \alpha \, \frac{\partial \cos \beta}{\partial x} + \cos \beta \, \frac{\partial \cos \beta}{\partial y} + \cos \gamma \, \frac{\partial \cos \beta}{\partial z} = -\frac{1}{\rho V^2} \frac{\partial p}{\partial y} \tag{18}$$

$$\cos \alpha \, \frac{\partial \cos \gamma}{\partial x} + \cos \beta \, \frac{\partial \cos \gamma}{\partial y} + \cos \gamma \, \frac{\partial \cos \gamma}{\partial z} = -\frac{1}{\rho V^2} \frac{\partial p}{\partial z} \tag{19}$$

## SOME PARTICULAR CASES

(a) The angle $\alpha$ is small, i.e., the direction of the velocity vector everywhere in the flow region nears the direction of $x$ = axis.

Supposing that $\cos \alpha = 1$ in Eqs. (18), (19), (10), and (4) we shall have the system of equations

$$\frac{\partial v}{\partial t} + v \frac{\partial v}{\partial y} + w \frac{\partial v}{\partial z} = -\frac{1}{\rho} \frac{\partial p}{\partial y} \tag{20}$$

$$\frac{\partial w}{\partial t} + v \frac{\partial w}{\partial y} + w \frac{\partial w}{\partial z} = -\frac{1}{\rho} \frac{\partial p}{\partial z} \tag{21}$$

$$\frac{\partial \rho}{\partial t} + \frac{\partial (\rho v)}{\partial y} + \frac{\partial (\rho w)}{\partial z} = 0 \tag{22}$$

$$\frac{\partial}{\partial t} \left( \frac{p}{\rho^\varkappa} \right) + v \frac{\partial}{\partial y} \left( \frac{p}{\rho^\varkappa} \right) + w \frac{\partial}{\partial z} \left( \frac{p}{\rho^\varkappa} \right) = 0 \tag{23}$$

where $t = x/V_{\max}$, $v = \cos \beta V_{\max}$, $w = \cos \gamma V_{\max}$. The system of Eqs. (20)–(23) fully coincides with the system of two-dimensional unsteady adiabatic motions of gas.

(b) The motion is two-dimensional, parallel, does not depend upon coordinate $z$, and potential. The range of the variation of the angles of the velocity vector inclination is not limited.

In the case being considered, Eq. (10) is presented in the form

$$\frac{\partial \ln \rho}{\partial \zeta} - \sin \alpha \, \frac{\partial \alpha}{\partial x} + \cos \alpha \, \frac{\partial \alpha}{\partial y} = 0 \tag{24}$$

It may also be presented as

$$\frac{\partial \ln \rho}{\partial \zeta} + \frac{\partial \alpha}{\partial n} = 0 \tag{25}$$

where derivative with respect to $\alpha$ means differentiation along the normal to the streamline.

The equation of the irrotational flow has the form

$$\frac{\partial(V \cos \alpha)}{\partial y} - \frac{\partial(V \sin \alpha)}{\partial x} = 0$$

It may also be presented as

$$\frac{\partial V'}{\partial n} - V \frac{\partial \alpha}{\partial \zeta} = 0 \tag{26}$$

where

$$V' = V_{max} - V$$

The Bernoulli-Sen-Vhenah Eq. (6) and the isentropic condition give for the whole flow region differential equation

$$V dV' = \frac{1}{\rho} dp \tag{27}$$

by means of which present Eq. (26) in the form

$$V^2 \frac{\partial \alpha}{\partial \zeta} = -\frac{1}{\rho} \frac{\partial p}{\partial n} \tag{28}$$

In Eqs. (25) and (28) change differentiation with respect to $\zeta$ and $n$ for differentiation with respect to potential $\varphi$ and stream functions $\psi$ for differential relations

$$d\varphi = \frac{V}{V_{max}^2} d\zeta; \qquad d\psi = \frac{V^{\cdot}}{V_{max}} \rho \, dn \tag{29}$$

The resultant equations system is

$$\frac{\partial \ln \rho}{\partial \varphi} + \rho \frac{\partial(\alpha V_{max})}{\partial \psi} = 0$$

$$\frac{V^2}{V_{max}^2} \frac{\partial(\alpha V_{max})}{\partial \varphi} = -\frac{\partial p}{\partial \psi} \tag{30}$$

Supposing in the coefficient of the left-hand side of Eq. (30) $V = V_{max}$ and introducing notation

$$W = \alpha V_{max} \tag{31}$$

present the system of Eqs. (30) in the form

$$\frac{\partial \ln \rho}{\partial \varphi} + \rho \frac{\partial W}{\partial \psi} = 0, \qquad \frac{\partial W}{\partial \varphi} = -\frac{\partial p}{\partial \psi} \tag{32}$$

The equations of the one-dimensional unsteady isentropic gas motion along the axis $\xi$ at a speed of $W(x_1 t)$ have the form

$$\frac{d \ln \rho}{dt} + \frac{\partial W}{\partial \xi} = 0, \qquad \frac{dW}{dt} = -\frac{1}{\rho} \frac{\partial p}{\partial \xi} \tag{33}$$

Replacing $\xi$ with Lagrange coordinate $m$ according to the formula

$$m = \int_{\xi_0(t)}^{\xi} \rho(\xi_1 t)\, d\xi \tag{34}$$

where $\xi_0(t)$ is value of $\xi$ for arbitrary fixed particle. Then the system [Eq. (33)] will be transformed into the system

$$\frac{\partial \ln \rho}{\partial t} + \rho \frac{\partial W}{\partial m} = 0, \qquad \frac{\partial W}{\partial t} = -\frac{\partial p}{\partial m} \tag{35}$$

The system of Eqs. (32) coincides with the system [Eq. (35)] if $\varphi$ is replaced with $t$ and $\psi$ with $m$.

We have considered steady flows when $V_{\max}$ is constant in the whole flow. If it varies from one stream to another, then using the condition of its constancy along the streamlines $dV_{\max}/dt = 0$, transform the system of the Eqs. (1)–(6) into the form

$$u_1 \frac{\partial u_1}{\partial x} + v_1 \frac{\partial u_1}{\partial y} + w_1 \frac{\partial u_1}{\partial z} = -\frac{1}{\rho_1}\frac{\partial p}{\partial x}$$

$$u_1 \frac{\partial v_1}{\partial x} + v_1 \frac{\partial v_1}{\partial y} + w_1 \frac{\partial v_1}{\partial z} = -\frac{1}{\rho_1}\frac{\partial p}{\partial y}$$

$$u_1 \frac{\partial w_1}{\partial x} + v_1 \frac{\partial w_1}{\partial y} + w_1 \frac{\partial w_1}{\partial z} = -\frac{1}{\rho_1}\frac{\partial p}{\partial z} \tag{36}$$

$$u_1 \frac{\partial}{\partial x}\left(\frac{p}{\rho_1{}^\varkappa}\right) + v_1 \frac{\partial}{\partial y}\left(\frac{p}{\rho_1{}^\varkappa}\right) + w_1 \frac{\partial}{\partial z}\left(\frac{p}{\rho_1{}^\varkappa}\right) = 0$$

$$\frac{\partial(\rho_1 u_1)}{\partial x} + \frac{\partial(\rho_1 v_1)}{\partial y} + \frac{\partial(\rho_2 w_1)}{\partial z} = 0$$

$$\frac{u_1{}^2 + v_1{}^2 + w_1{}^2}{2} + \frac{\varkappa}{\varkappa - 1}\frac{p}{\rho_1} = \frac{V_{\max_1}{}^2}{2} = i_{0_1}$$

where

$$u_1 = V_0 \frac{u}{V_{\max}}, \qquad v_1 = V_0 \frac{v}{V_{\max}}, \qquad w_1 = V_0 \frac{w}{V_{\max}}$$

$$\rho_1 = \rho\phi \frac{V_{\max}{}^2}{V_0{}^2}, \qquad V_{\max_1}{}^2 = V_0{}^2 = \text{Const.}$$

$V_0$ is a constant which has the velocity dimension. In the obtained equivalent flow the value of the maximum velocity is constant everywhere. Present entropic function of the equivalent flow in the form

$$\frac{p}{\rho_1{}^\varkappa}, \qquad V\frac{p}{(\rho{}^i{}_0/i_{0_1})}, \qquad \varkappa = \frac{p}{(\rho T_0/T_{0_1})}, \qquad \varkappa = \frac{p_0}{(\rho_0 T_0/T_{0_1})}, \qquad \varkappa = (RT_{0_1})^z\, p_1{}^{1-z}$$

where $T_0$ is the initial flow stagnation temperature which is varied from one line stream to another, $T_{0_1} = i_{0_1}/J_{c_0}$ is the equivalent flow stagnation temperature, which is constant everywhere, and $p_0$ is the initial flow stagnation pressure.

Thus the equivalent flow is isentropic if the initial flow stagnation pressure is constant everywhere. In this case this equivalent flow is irrotational because its entropy and enthalpy are constant. The given consideration allows to use the above-mentioned cases (a) and (b) in the equivalent flow.

In this case bear in mind that if the initial flow is hypersonic then the equivalent flow is also hypersonic because the distribution of the local $M$ numbers in these two flows coincides.

Equations (1)–(5) permit exact solution where $p \equiv 0$, $\rho \neq 0$, $V$ is finite. It ensues from Eqs. (1)–(3) that $dV/dt = 0$, where $V$ is the velocity vector. This shows that all stream lines are straight and that the velocity value on each stream is constant. Local $M$ numbers are equal to infinity. There is no interaction between the particles, and they expand by inertia. It is of interest to consider such flows.

Proceeding from more complicated premises, the author of Ref. 5 has come to such a kind of flows. The unsteady analogy of case (a) gives unsteady expansion by inertia in the space of smaller numbers of dimensions.

The analogy of case (a) allows the creation of steady hypersonic flows in the nozzles and diffusers of the particular kind derived from exact solutions of unsteady equation of the gas dynamics with the control symmetry, corresponding to some motions of gas, for which the velocity distribution in each moment of time linearity depends on the distance from the symmetry center. The solutions are obtained by L. I. Sedov, who gives them in the form of Ref. 6.

$$dt = \pm \frac{d\mathfrak{M}}{\mathfrak{M}^2 \left[A + B\mathfrak{M}^{\nu(\varkappa-1)}\right]^{1/2}} \tag{37}$$

$$\frac{dr}{dt} = v = -\frac{1}{\mathfrak{M}}\frac{d\mathfrak{M}}{dt} \qquad r = \pm \mathfrak{M}\sqrt{A + B\mathfrak{M}^{\nu(\varkappa-1)}}\, r \tag{38}$$

$$\rho = \mathfrak{M}^{\partial}(r\mathfrak{M})^s P'\left[(r\mathfrak{M})^{s+2}\right] \tag{39}$$

$$p = \mathfrak{M}^{\varkappa v}\left\{c + \frac{(x-1)^s}{2(s+2)} BP\left[(r\mathfrak{M})^{s+2}\right]\right\} \tag{40}$$

Where $r$ is the distance from the center of the symmetry, $A$, $B$, $c$, $s$ are arbitrary constants. $P$ is the arbitrary function of the argument.

Value $s = 1$ for two-dimensional symmetry, $s = 2$ for cylindrical symmetry, $s = 3$ for spherical symmetry.

Show that among solutions expressed by Eqs. (37)–(40) there are isentropic ones, which are of great interest for our purposes. These solutions do not contain arbitrary function and are determined by the system of the equations

$$dt^2 = t_0^2 \frac{d\xi^2}{\epsilon_1 + \epsilon_2 \xi^{2k/(2+k)}} \tag{41}$$

$$a^2 = \epsilon_1 \frac{\varkappa - 1}{2} \frac{k}{2} \left(\frac{2}{2+k}\right)^2 \frac{r_0^2}{t_0^2} (R^2 + \epsilon_3)\xi^{-2k/(2+k)} \tag{42}$$

$$v^2 = \left(\frac{2}{2+k}\right)^2 \frac{r_0^2}{t_0^2} R^2 \xi^{-2k/(2+k)} (\epsilon_1 + \epsilon_2 \xi^{2k/(2+k)}) \tag{43}$$

$$R = \frac{r}{r_0} \xi^{-2k/(2+k)} \tag{44}$$

In this case $k = \nu(\varkappa - 1)$, $r_0$, $t_0$ are arbitrary constants with dimensions of length and time, $\epsilon_1$, $\epsilon_2$, $\epsilon_3$ may assume meaning $+1$ and $-1$ independently of each other. In each combination of parameters and signs this solution is suitable only if the right-hand sides of Eqs. (41)–(43) are positive.

The differential equations of two families of characteristics

$$\frac{dr}{dt} = v \pm a \tag{45}$$

are integrated. With $\epsilon_1 = +1$ the characteristics equations are

$$(R + \sqrt{R^2 + \epsilon_3})^{2\sqrt{\nu}} \frac{1 + \sqrt{1 + \epsilon_2 \xi^{2k/(2+k)}}}{1 - \sqrt{1 + \epsilon_2 \xi^{2k/2+k}}} = H_2 = \text{Const.} \tag{46}$$

$$(R + \sqrt{R^2 + \epsilon_3})^{2\sqrt{\nu}} \frac{1 - \sqrt{1 + \xi^{2k/(2+k)}}}{1 + \sqrt{1 + \xi^{2k/(2+k)}}} = H_2 = \text{Const.} \tag{47}$$

The characteristic equations with $\epsilon_1 = -1$ have the form

$$\arcsin R - \frac{1}{\sqrt{\nu}} \arccos \xi^{-k/(2+k)} = N_1 = \text{Const.} \tag{48}$$

$$\arccos R + \frac{1}{\sqrt{\nu}} \arccos \xi^{-(k)/(2+k)} = N_2 = \text{Const.} \tag{49}$$

Turning to the equivalent hypersonic flow in accordance with the case $(a)$, $\bar{\varkappa} = x/r_0$ assume that $t = x/V_{\max}$, $r_0/t_0 = V_{\max}$, $\bar{\epsilon} = r/r_0$, $V_{\max}$ is the constant value of the maximum velocity.

Equations (41)–(44) have the form

$$d\bar{x}^2 = \frac{d\xi^2}{\epsilon_1 + \epsilon_2 \xi^{2k/(2+k)}} \tag{50}$$

$$a^2 = \frac{\varkappa - 1}{2} \frac{k}{2} \left(\frac{2}{2+k}\right)^2 V_{\max} (R^2 + \epsilon_3) \xi^{-2k/(2+k)} \tag{51}$$

$$R = \bar{r} \, \xi^{-2k/(2+k)} \tag{52}$$

$$v^2 = \left(\frac{2}{2+k}\right)^2 V_{max}^2 \, R^2 \xi^{-2k/(2+k)} \left(\epsilon_1 + \epsilon_2 \, \xi^{2k/(2+k)}\right) \tag{53}$$

Equations (46)–(49) of the characteristics will be of the same kind. For the local Mach numbers of the flow we have the equations

$$M^2 = \frac{V_{max}^2}{a^2} = \pm \frac{1}{\varkappa - 1} \frac{1}{k} (2 + k)^2 \frac{\xi^{2k/(2+k)}}{R^2 + \epsilon_3} \tag{54}$$

If $\epsilon_3 = +1$ then Mach number $M_0$ on the symmetry axis (with $R = 0$) will be

$$M_0 = \frac{2 + k}{\sqrt{(\varkappa - 1)k}} \, \xi^{k/(2+k)}$$

The distribution of Mach number along $R$ with $\xi$ fixed will be

$$\frac{M}{M_0} = \frac{1}{R^2 + 1}$$

With $R = 1$ the Mach number is twice less than on the axis. The creation of such flows with the nonuniform Mach number along the section may allow to obtain higher Mach numbers near the symmetry axis with not very high Mach numbers along the section. If $\epsilon_3 = -1$ and $\epsilon_1 = +1$ then the flow exists only at $R > 1$, $R = 1$, $a = 0$, $M = \infty$. In the zone of $R < 1$, $a \equiv 0$ there is a high vacuum. The relation [Eq. (53)] with $R$ fixed is an equation of stream lines. Any of them may be chosen as a hard wall and one can consider the flow in the region of smaller values of $R$.

In this case the values $\xi$ and $x$ are related by Eq. (50). Thus quite identical distributions of Mach numbers along $R$, determining the relation [Eq. (54)] are obtained at quite different stream lines.

The relation [Eq. (52)] may be presented in the form

$$\alpha = \frac{2}{2+k} \, R \xi^{-k/(2+k)} \sqrt{\epsilon_1 + \epsilon_2 \, \xi^{2k/(2+k)}} \tag{55}$$

where $\alpha = v/V_{max}$ approximate value of the velocity vector inclination angle to the $X$ axis. At $\epsilon_1 = \epsilon_2 = 1$ and $R = $ Const. $\xi \to \infty$ the value $\alpha$ tends to $2/(2+kR)$

When increasing the motion transforms into the motion with straight stream lines, which are trajectories of the gas particles motion by inertia. In this case Eqs. (46) and (47) of the characteristics give when $\xi \to \infty$ quite definite values of $R$, which is in complete agreement with Ref. 5 results as to possibility of the infinite influence regions for bounded domains in hypersonic flows. It is interesting that density distribution across the flow remains uniform.

At $\epsilon_1 = 1$, $\alpha = 0$, $\epsilon_2 = -1$ when $\bar{x} = \bar{x}_1$ corresponding to the value of $\xi = 1$. We have hypersonic nozzle with constant decrease of the stream lines inclination to the $X$ axis up to zero.

The neighborhood of the point, corresponding to values, $\bar{x} = \bar{x}_1$, $R = 0$, under some conditions may be used as the "test section" of the hypersonic wind tunnel. The flow can be reflected symmetrically to the plane $\bar{x} = \bar{x}_1$ and then down stream from this section there will be a hypersonic diffuser.

One can try first to boost the flow in the usual conical nozzle and then boost it under conditions of transforming the flow into the flow considered above.

To find the nozzle contours, which give such a transition, it is necessary to solve, for example, using the characteristics method, a problem of the Goursat type problem of determination of the flow according to data on two characteristics, resulting from a point on the symmetry axis. In this case the characteristics equations found above can be of use.

## REFERENCES TO PART I

1. Hsue-shen, Tsien, "Similarity Laws of Hypersonic Flows," *J. Math. Phys.*, vol. 25, no. 3, 1946.
2. Hayes, Wallace D., "On Hypersonic Similitude," *Quart. Appl. Math.*, vol. 5, no. 1, April 1947.

# PART II*

## WAVE STARTING OF THE SUPERSONIC AND HYPERSONIC DIFFUSER

In the usual starting of the supersonic wind tunnel with fixed supersonic diffuser the shock wave is moved from the critical nozzle area in the direction of the test section when the ratio of the stilling chamber pressure to the pressure in the end of the subsonic part of the diffuser is increased and maximum total pressure losses in the shock determine the ranges of possible supersonic diffuser throat area. If the gas friction at the walls is not considered, then the maximum regime is determined by the relation

$$F_{*g}/F_{*c} = 1/\nu_{nc} \qquad (56)$$

where $F_{*g}$ = critical throat area of the diffuser, $F_{*c}$ = critical nozzle area, and $\nu_{nc} = p_0'/p_0$ is the ratio of total pressure (the pressure of the adiabatic stagnation) after the normal shock, according to calculated Mach number in the working section, to total pressure $p_0$ before it. In this case the condition of creation of the supersonic regime in the wind-tunnel operation section can be written in the form

$$F_{*g}/F_{*c} > \frac{1}{\nu_{nc}} \qquad (57)$$

If this condition is not held, then at some value of the ratio $\epsilon = p_T/p_k$ (the pressure $p_T$ in the stilling chamber to the pressure $p_k$ in the end of the subsonic part of the diffuser) in the diffuser throat, the velocity equal to local sound speed is established, the diffuser is "choked," and the shock is fixed in a certain section of the nozzle, without reaching the working section. The supersonic flow in the working section cannot be created by any further increase in the ratio of $\epsilon = p_T/p_k$.

If this condition [Eq. (57)] is held, then at $\epsilon = p_T/p_k = 1/\nu_{nc}$ the shock suddenly moves down stream through the diffuser throat up to the section, where the Mach number of the supersonic stream is equal to the Mach number in the working section. In fact, due to the boundary layer on the walls of the nozzle and diffuser and its interaction between shocks, the above-described phenomena occur, but in different limits of parameter values. After the shock has moved through the diffuser throat and the supersonic flow is formed in and in front of it, the supersonic flow is decelerated more in the converging part of the diffuser by decreasing the diffuser throat almost up to the flow breakdown. Then the value $\epsilon$ is decreased almost up to the limiting value, corresponding to the sudden shock-wave movement to the nozzle, which is accompanied with the supersonic flow breakdown in the working section.

In the supersonic and hypersonic wind tunnels with circular working sections and especially with short running time, the adjustment of the diffuser at starting to obtain the optimal operation regime is associated with great construction difficulties in geometry and decrease in the wind tunnel running time. This is

---

* With A. Y. Lashkov.

why methods of starting the fixed supersonic diffuser to obtain optimal operation regime without any adjustment are of obvious interest. One of such starting methods—rejection of the part of flow at the diffuser inlet—was proposed by Eggink in 1953.[1]

The method of supersonic diffuser starting in which pecularities of the unsteady flow are used is outlined in the present paper.

The same steady-gas flows can be "constructed" in time and space by different ways depending on their formation "history." The usual method of optimal supersonic diffuser starting previously described can be used to "construct" the supersonic flow in the diffuser. The method is reduced to the successive change of steady flows with normal shocks in the nozzle working section and diffuser system.

The present paper is based on the following principle of construction of steady supersonic flow in the nozzle working section and diffuser system. The supersonic flow is formed by means of some unsteady gas dynamic wave process which is not due to the change of the steady motions; this accounts for the fact that it is quite free of the geometric restrictions, expressed by relations of the type [Eq. (57)] which are the steady flow properties. This unsteady motion in the ideal case can be considered as follows.

Let a diaphragm be set in the nozzle critical area. Then from one side of it—in the stilling chamber and subsonic part of the nozzle—let the gas be at rest with some values of the pressure and density. From its other side—the supersonic nozzle, working section, supersonic and subsonic diffusers—is the vacuum. Let the diaphragm disappear at some initial moment of time $\tau = 0$.

Then at $\tau > 0$ there will appear an unsteady wave motion in the gas, coterminal to the vacuum; with this motion the expanding gas will tend to become a vacuum with supersonic speeds. First through the nozzle, working section and diffuser unsteady supersonic gas will pass, then this unsteady motion will be transformed quickly but continuously into the calculated steady supersonic flow. If the nozzle is hypersonic, then the volume of the exhaust gas will expand with time region of steady flow coterminal to the vacuum through the thin layer of the wave motion (Rhiman expansion-wave type). For steady hypersonic flows, if the angles of the velocity vector inclination to a certain fixed direction are small, the hypersonic similitude law is valid. That is why at the gas expansion into the nozzle diffuser system, designed for obtaining hypersonic speeds, the fixed-plane gas elements, normal to the wind-tunnel axis, will move and deform independently of each other, while their axis velocity is hypersonic. From the point of view of the application of the hypersonic similitude law even Mach numbers $M = 2.5$–$3$ for air are hypersonic.

This consideration shows that in hypersonic wind tunnels it is always possible, using the recommended method, to start the fixed diffuser, decreasing any hypersonic Mach number to $M = 3$. Practically, it is apparent, that at sufficiently high Reynolds numbers and reasonable geometry it is possible to start the hypersonic diffuser, decreasing the Mach numbers almost up to $M = 1$ and thus limitations in the hypersonic diffuser efficiency pertain not to its starting, but to the possible existence in it of the steady supersonic flow of viscous gas.

Evidently the process will approximate the described one if at the initial moment $\tau = 0$ in the supersonic nozzle-working section-diffuser system the vacuum is not high and there is a gas with a small ratio of pressure and density to their values for the high-pressure gas, which is on the other side of the nozzle critical area.

## EXPERIMENTAL INSTALLATION

A model of intermittently operating supersonic wind tunnel was used as an experimental installation; its general view and schematic diagram are given in Figs. 1 and 2.

The aerodynamic contour of the tunnel model is quite simple, the straight supersonic nozzle having the expansion angle of $7°20'$; the initial nozzle area (in which the diaphragm installed) being $5 \times 30$ mm and the working section area $F_2 = 19.30 \times 30$ mm.

The Mach number calculated for air by the formulas of gas dynamics at the nozzle exit corresponded to the value of $M = 2.905$.

The supersonic diffusers Nos. 1, 2, 3 were changeable and had the following nozzle throat-to-maximum area ratios respectively: $h = 0.57$, $h = 0.415$, and $\bar{h} = 0.31$. The expansion angle of the diffuser supersonic part for variants of diffusers Nos. 1 and 3 was the same and equal to $\theta = 16°$, and for the diffuser No. 2, $\theta = 17°$. Expansion angle of the subsonic diffuser in all variants was equal
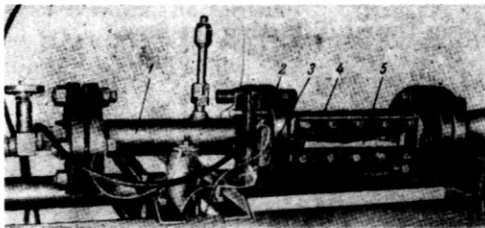


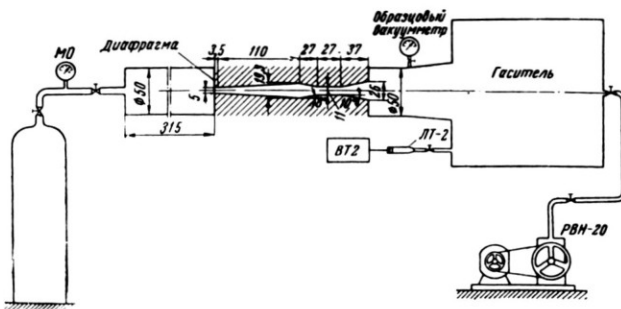Fig. 1. (1) Stilling section; (2) start sensor; (3) diaphragm section; (4) working section; (5) diffuser.



Fig. 2. (1) Diaphragm; (2) reference vacuum meter; (3) damper (vacuum).

to $\alpha = 18°$. The operating process of the installation (Figs. 1 and 2) with time was the following:

1. pumping out the damper by PBH–20 vacuum pump till the designed pressure, which was measured by the BT–2 device or reference vacuum-meter

2. opening of the bottle valve and gradual increase of the initial pressure in the stilling chamber

3. diaphragm break

4. starting of the time delay system, set beforehand for a definite period of $\tau$ $\mu$sec by a piezosenser

5. after $\tau$ $\mu$sec, firing of spark device and taking pictures of flow using the IAS-451 shadow device.

To check the proper record of the test time, the delay of $\tau$ $\mu$sec and the flash moment are fixed on the oscillograph.

The knife edge of the shadow device during all the tests was in the vertical position (longitudinal gradient).

At a pressure of 6 kg/cm² one cellophane diaphragm $\delta = 0.04$ mm wide was used. At a pressure about 15 kg/cm² two cellophane diaphragms $\delta = 0.04$ m wide each were used, and at a pressure of 60 kg/cm² one brass diaphragm $\delta = 0.03$ mm wide was used.

The spark filming duration before the tests was checked by CΦP–2M device and did not practically exceed 1 $\mu$sec. Air was used as working gas in the first group of tests, then nitrogen was used, since the air humidity caused condensation shocks in the diffuser throat distorting the flow.

## TEST RESULTS

The performed tests were in the main of qualitative character, since the principal aim was to confirm experimentally the general theoretical considerations about the possibility of "starting" optimal supersonic diffusers, using the method proposed in this paper. The problem determined the methods for performing the test.

A picture of the gas flow was obtained in the nozzle and diffuser of straight aerodynamic contours.

During creation of the supersonic flow, one may expect that it is easily formed in a more perfect aerodynamic contour of the channel.

As it was stated above, three diffusers were used during the test. Diffuser No. 1 had a relative throat area of $\bar{h} = 0.57$.

For Mach number in working section equal to $M = 2.905$ by the theoretical hydraulic formula[2] and according to Hermann experimental data[2] the minimum relative area of the supersonic diffuser throat at which the latter is started in a usual way, $h = 0.72$.

The spark photographs (Figs. 3–5) show the sequential development of the flow at starting of the intermittent supersonic diffuser No. 1.

As may be seen on the photographs, this diffuser with the throat area considerably decreased was started and continuously operated practically during the calculated period of the installation operation.

Figure 3 fixes the flow picture in $\tau = 250$ $\mu$sec after the diaphragm breakage at a pressure in the damper of $p_k = 0.0003$ kg/cm$^2$ and pressure in stilling chamber of $p_T = 16$ kg/cm$^2$.

In this case the products of the cellophane diaphragm are seen breaking in supersonic nozzle exit. At this moment supersonic flow and oblique shocks appeared in the diffuser.

The spark photographs of Figs. 4 and 5 show the flow spectrums in 3500 and 10000 $\mu$sec respectively, after the diaphragm opening at the same values of $p_k$ and $p_T$. The flows represented in these two photographs are uniform and identical. The flows of Fig. 3 greatly differ from those of Figs. 4 and 5. The much greater inclination angle of oblique shocks, to the diffuser walls in Fig. 3 than in Figs. 4 and 5, shows that with $\tau = 250$ $\mu$sec the flow of gas at the end of the nozzle and in the diffuser is still unsteady and Mach number is much higher than the calculated one. The inclination angle of the oblique shocks at the diffuser inlet in Figs. 4 and 5 rises up to $\gamma = 30°$ and this corresponds approximately to the calculated regime of the flow $M_2 = 2.9$. The coincidence of the flows in Figs. 4 and 5 shows that they correspond to the steady motion of the gas in the nozzle and diffuser.

The experiments with diffuser 1 were repeated under gradual increase of pressure $p_*$ in the damper.

There was steady flow after the unsteady starting in the experiment with $p_T = 15$ kg/cm$^2$ and $p_k = 0.125$ kg/cm$^2$, and this corresponds to the range of the ratio $p_T/p_k > 120$.
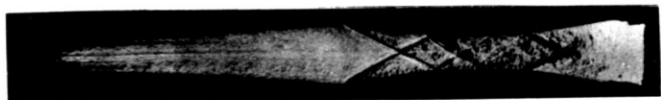


Fig. 3. $\bar{h} = 0.72$; $\tau = 250$ $\mu$sec.



Fig. 4. $\bar{h} = 0.72$; $\tau = 3,500$ $\mu$sec.



Fig. 5. $\bar{h} = 0.72$; $\tau = 10,000$ $\mu$sec.

Diffuser 2 was half shorter than diffuser 1, and the former had the relative area of the throat, $\bar{h} = 0.415$ equal to the optimum one, received in the paper[2] for the diffuser with the adjustable walls with $M = 2.9$. The spectrum spark photograph of the flow in diffuser 2 after the starting at the beginning of the steady stage, is given in Fig. 6. The stability of the steady flow in the diffuser 2 within the precision of the experiment was exactly the same as in diffuser 1.

Diffuser 3 had the relative area $\bar{h} = 0.31$ similar to the value $h = 0.28$ for isentropic flow with $M_2 = 2.9$.

The diffuser was started (Fig. 7) and this you can see on the spark photograph taken in $\tau = 400$ $\mu$sec after opening of the diaphragm with $p_T = 50$ atm and $p_k = 0.0003$ atm.

The inclination of oblique shocks at the diffuser inlet corresponds to the calculated regime of the flow $M_2 = 2.9$.

However, in 180 $\mu$sec the supersonic flow in the diffuser was broken down and in 3800 $\mu$sec became typical of the choking regime of the supersonic diffuser (Fig. 9).

Thus, by means of the unsteady flow regime the supersonic diffuser can be started even with the throat area nearly equal to the supersonic nozzle critical area, but the duration of work of such a diffuser will be very short, as it is impossible to have a steady flow in such a diffuser. Probably the flow is broken down because of rapid increase of the boundary layer which interacts with oblique shocks.

The spark photographs of Figs. 10–14 are taken approximately in $\tau = 250$ $\mu$sec after the break of the cellophane diaphragm of $\delta = 0.04$ mm thickness, placed in the throat of the supersonic nozzle.

The flow spectrum at the moment of the optimum supersonic diffuser starting at $p_T = 17.6$ atm, $P_k = 0.0526$ atm, $p_T = 18$ atm, $p_k = 0.0856$ is given in Figs. 10–11. The spectrum of the development of this flow with time — in 800 $\mu$sec is given on Fig. 11a.

Figures 12–14 illustrate change in character of a number of unsteady flows in case of successive increase in $P_k$; $P_k = 0.0985$ atm, $P_k = 0.207$ atm, $P_k = 0.446$ atm.



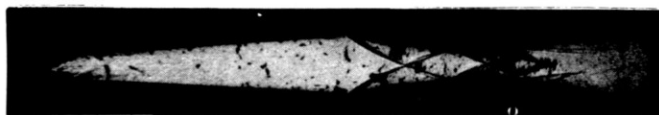Fig. 6.   $\bar{h} = 0.415$.


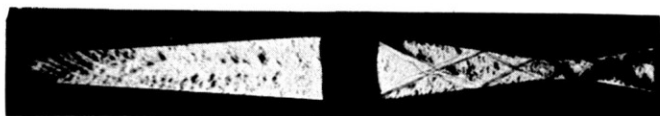
Fig. 7.   $\bar{h} = 0.31$; $\tau = 400$ $\mu$sec.
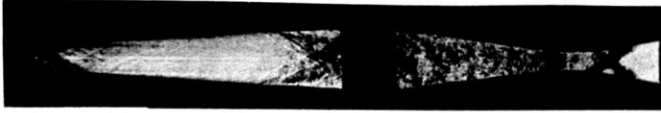
Fig. 8.  $\bar{h} = 0.31$; $\tau = 480$ $\mu$sec.



Fig. 9.  $\bar{h} = 0.31$; $\tau = 3,800$ $\mu$sec.



Fig. 10.  $\bar{h} = 0.415$; $\tau = 250$ $\mu$sec; $P_0 = 17.6$ $at$; $p_k = 0.0526$.



Fig. 11.  $\bar{h} = 0.415$; $\tau = 250$ $\mu$sec; $P_0 = 18$ $at$; $p_k = 0.0856$ $at$.



Fig. 11a.  $\bar{h} = 0.415$; $\tau = 800$ $\mu$sec; $P_0 = 18$ $at$; $p_k = 0.0856$ $at$.



Fig. 12.  $\bar{h} = 0.415$; $\tau = 250$ $\mu$sec; $P_0 = 18$ $at$; $p_k = 0.0985$ $at$.
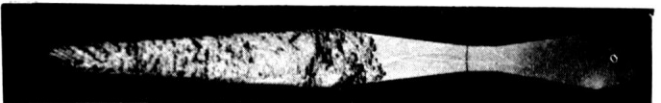


Fig. 13.  $\bar{h} = 0.415$; $\tau = 250$ $\mu$sec; $P_0 = 18$ $at$; $p_k = 0.207$ $at$.

The specter of flow, shown in Fig. 14, does not differ practically from that obtained when photographing the unsteady expansion into atmosphere under the same conditions (Fig. 15).

By increasing the pressure in the damper, $P_k$, at $p_T$ = Const., sufficient for maintaining the steady flow in the hypersonic diffuser, we change for a quite definite kind of unsteady flow, at which the hypersonic diffuser cannot be started.

The process development of this unsteady flow in the fixed nozzle-operating part-diffuser system, is shown in Fig. 15a through $f$.

The flash photographs are taken at $p_T$ = 16 atm, $P_k$ = 1 atm starting with $\tau$ = 100 $\mu$sec after the cellophane diaphragm is broken $\delta$ = 0.04 mm in succession after every 50–100 sec.

The physical picture of development of this kind of unsteady flow is characterized by the presence of a zone of vividly expressed turbulent flow structure—contact discontinuity type, moving after a comparatively uniform region, which follows the shock wave, after the diaphragm is broken.

Formation of cross waves and their interaction with the incident shock wave is clearly seen in the photos. The turbulent region of the flow gradually filling ($\tau$ = 100:350 $\mu$sec) the whole visible flow region is characterized by a high-density gradient in the longitudinal and lateral directions. It is clearly seen on Fig. 15, where the flow spectra is photographed after $\tau$ = 400 $\mu$sec, with the Foucault knife edge fully removed.

As is seen from the above, the flow in the turbulent region is subsonic. The hypersonic region, which formed after the nozzle critical area in $\tau$ = 400 $\mu$sec is bounded by a system of oblique shocks ($m$), which is followed by the flow separation; the stream, formed in the center, still keeps the hypersonic speed, but at a certain distance is ended in a normal shock, $n$. Next the unsteady pulsating subsonic flow enters the hypersonic diffuser, where it accelerates up to the sound speed in the diffuser throat, and becomes more uniform under negative pressure-gradient influence.

The hypersonic flow region, which formed after the hypersonic diffuser throat, is practically free from turbulent pulsations.

The idea of the supersonic diffuser starting under the conditions of preliminary pumping out of gas between the nozzle critical area and the diffuser critical area was checked. The supersonic nozzle, calculated by the gas hydraulic formulas has a Mach number $M$ = 4.5 for $\varkappa$ = 1.4, the relative area of the hypersonic diffuser being $\bar{h}$ = 0.2.

After the supersonic diffuser two cellophane diaphragms $\delta$ = 0.04 m wide were installed. The working section of the nozzle up to the throat area and supersonic diffuser were previously pumped out with a vacuum pump up to a pressure of $P_k$ = 0.0001 atm, Figs. 16, 16a; $P_k$ = 0.001 atm. Fig. 16b; $P_k$ = 0.16 atm, Fig. 16c.

Pressure of $P_T$ = 60 atm in the stilling chamber was maintained constant. After the diaphragm was broken expansion into the damper took place; the damper pressure was equal to atmospheric.

Fig. 14. $\bar{h} = 0.415$; $\tau = 250 \,\mu\text{sec}$; $P_0 = 18 \,\alpha t$; $p_k = 0.446 \,\alpha t$.



Fig. 15a. $\bar{h} = 0.415$; $\tau = 100 \,\mu\text{sec}$; $P_0 = 16 \,\alpha t$; $p_k = 1 \,\alpha t$.



Fig. 15b. $\bar{h} = 0.415$; $P_0 = 16 \,\alpha t$; $p_k = 1 \,\alpha t$.



Fig. 15c. $\bar{h} = 0.415$; $P_0 = 16 \,\alpha t$; $p_k = 1 \,\alpha t$.



Fig. 15d. $\bar{h} = 0.415$; $P_0 = 16 \,\alpha t$; $p_k = 1 \,\alpha t$.
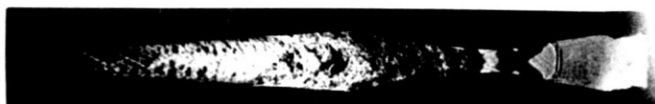


Fig. 15e. $\bar{h} = 0.415$; $P_0 = 16 \,\alpha t$; $p_k = 1 \,\alpha t$.



Fig. 15f. $\bar{h} = 0.415$; $P_0 = 16 \,\alpha t$; $p_k = 1 \,\alpha t$.

The flow process with $P_k$ = Const. was photographed in $\tau$ = 300 $\mu$sec since the moment of the diaphragm opening installed in the nozzle throat area, with the flash light used, Foucault knife edge was installed in vertical position (longitudinal density gradient).

Besides, using the device comprising the pulsing flash source, Teppler type, and photoregister with a linear speed of film equal to 0, 11 mm/$\mu$sec the diffuser development flow in time was photographed.

Flash photographs (Figs. 16 and 16a) illustrate the flow spectra in 100 and 300 $\mu$sec correspondingly, after the diaphragm breakage at $p_\mathrm{T}$ = 60 atm and $P_k$ = 0.0001 atm, showing the starting of hypersonic diffuser at $M$ = 4.5. The flow illustrated in Fig. 16 differs from that in Fig. 16a by the great inclination of oblique shocks to the diffuser walls which indicates the unsteady character of the flow at $\tau$ = 100 $\mu$sec. Mach number in this case is considerably greater than the calculated one.

An increase in pressure $P_k$ to 0.16 atm ($\tau$ = 300 $\mu$sec since the moment of the diaphragm breaking) considerably changes the flow character.

The flow regime fixed in the photograph of Fig. 16b is typical of the case of chocking. The similar flows are given in Figs. 14 and 15d. The film shot at $P_\mathrm{T}$ = 60 atm and $P_k$ = 0.00001 atm is an addition to the flows illustrated in Figs. 16a and 16b. The quasi-stationary flow duration in the hypersonic diffuser after the start was determined by the film and did not exceed 1,300 $\mu$sec. This period of time approximately corresponds to the calculated period determined by the losses in the flow of mechanical energy, in the device for the given case.

Starting of the supersonic diffuser under the conditions of pumping out of the nozzle and diffuser working section may be put into practice where great vacuum capacities are not available.



Fig. 16.   $\bar{h}$ = 0.2; $\tau$ = 100 $\mu$sec; $P_0$ = 60 $\alpha t$; $p_k$ = 0.0001 $\alpha t$.



Fig. 16a.   $\bar{h}$ = 0.2; $\tau$ = 300 $\mu$sec; $P_0$ = 60 $\alpha t$; $p_k$ = 0.001 $\alpha t$.



Fig. 16b.   $\bar{h}$ = 0.2; $P_0$ = 60 $\alpha t$; $p_k$ = 0.16 $\alpha t$.

# REFERENCES TO PART II

1. Eggink, H., "The Improvement in Pressure Recovery in Supersonic Wind Tunnels," Great Britain, Aeronautical Research Council, Reports and Memoranda No. 2703, 1953, May 1949.

2. German, R., Sverkhzvukovye vkhodnye diffuzory. Fizmatgiz, Moskva, 1960. (Translated from English language original: Hermann, Rudolf: "Supersonic Inlet Diffusers and Introduction to Internal Aerodynamics," Minneapolis, Minneapolis-Honeywell Regulator Co., Aeronautical Division, 1956.